INTERNATIONAL
Agrophysics
www.international-agrophysics.org

Int. Agrophys., 2020, 34, 409-423
doi: 10.31545/intagr/12754

Carbon consumption of developing fruit and the fruit bearing capacity of individual RoHo 3615 and Pinova apple trees**

Martin Penzel[1,2], *Alan Neil Lakso*[3], *Nikos Tsoulias*[1,4], *and Manuela Zude-Sasse*[1]*

[1]Department of Horticultural Engineering, Leibniz Institute for Agricultural Engineering and Bioeconomy (ATB), Germany
[2]Agromechatronics – Sensor-based Process Management in Agriculture, Technische Universität Berlin, Germany
[3]Horticulture Section, Cornell AgriTech, Cornell University, Geneva, NY 14456, USA
[4]Department of Natural Resources Management and Agricultural Engineering, Agricultural University of Athens, Greece

Received July 17, 2020; accepted September 3, 2020

Abstract. This paper describes an approach to estimate the photosynthetic capacity and derive the optimum fruit number for each individual tree, in order to achieve a defined fruit size, which is named as the fruit bearing capacity of the tree. The estimation of fruit bearing capacity was carried out considering the total leaf area per tree as measured with a 2-D LiDAR laser scanner, LA_{LiDAR}, and key carbon-related variables of the trees including leaf gas exchange, fruit growth and respiration, in two commercial apple orchards. The range between $^{min}LA_{LiDAR}$ and $^{max}LA_{LiDAR}$ was found to be 2.4 m² on Pinova and 4.3 m² on RoHo 3615 at fully developed canopy. The daily C requirement of the growing fruit and the associated leaf area demand, necessary to meet the average daily fruit C requirements showed seasonal variation, with maximum values in the middle of the growing period. The estimated fruit bearing capacity ranged from 33-95 fruit tree^{-1} and 45-121 fruit tree^{-1} on the trees of Pinova and RoHo 3615, respectively. This finding demonstrates sub-optimal crop load at harvest time in both orchards, above or below the fruit bearing capacity for individual trees. In conclusion, the LiDAR measurements of the leaf area combined with a carbon balance model allows for the estimation of fruit bearing capacity for individual trees for precise crop load management.

Keywords: fruit growth rate, fruit respiration, leaf area, LiDAR, precision horticulture

INTRODUCTION

As a perennial plant, the production of premium size apples requires a balance of crop level and the ability of the tree to support the crop as well as flower bud development for the following year. Crop load management (CLM) targets the fruit number per tree to enable the growth to optimal fruit sizes by optimizing the carbon supply to demand balance for economically desirable fruit growth. Also, when performed less than 30 days after full bloom, CLM avoids a reduction in flower bud development to prevent alternate bearing on susceptible cultivars (Kofler *et al*., 2019). CLM may include pruning to reduce flower-bud numbers per branch (Breen *et al*., 2015), mechanical (Penzel *et al*., 2021) or chemical thinning of flowers (Janoudi and Flore, 2005) or fruitlets (Penzel and Kröling, 2020), and frequently corrective hand thinning after fruit drop.

In order to optimize CLM for the quantity of profitable fruit size, it is crucial to define the optimum fruit number per tree, which should be considered as the target fruit number for the purposes of making an accurate determination of the intensity of each individual management practice (Treder, 2008; Robinson *et al*., 2017). The optimum fruit number per tree depends on the economically desirable fruit size at harvest, the daily C demand of growing fruit required to achieve this fruit size and the individual photosynthetic capacity of each tree to support fruit growth versus vegetative growth and flower bud development.

*Corresponding author e-mail: mzude@atb-potsdam.de
**This work was funded by the Ministry of Agriculture, Environment and Climate Protection of the federal state of Brandenburg and the agricultural European Innovation Partnership (EIP-AGRI), grant number 80168342 (2016-2020).

The photosynthetic capacity of fruit trees is associated with the extent of their generative and vegetative growth, both directly and indirectly determined by interacting factors of intra-plant competition. Furthermore, external factors such as light availability and interception, temperature, mineral nutrition, soil properties and water availability affect the photosynthetic capacity (Monteith, 1977; Xia *et al*., 2009; Lakso and Goffinet, 2017; Lopez *et al*., 2018). Physiological crop models can quantify cumulative effects of several factors on the magnitude of vegetative and generative growth of fruit trees (Lakso *et al*., 2001; Mirás-Avalos *et al*., 2011; Pallas *et al*., 2016). Therefore, physiological crop models are helpful in understanding the seasonal growth patterns of fruit trees or they may be used to determine the tree's photosynthetic capacity and they can also be applied as a tool for decision support for precise orchard management (Lakso and Robinson, 2014).

Furthermore, physiological and decision support models may be utilized to predict the optimum timing for the application of thinning agents (Robinson *et al*., 2017; Yoder *et al*., 2013), the thinning response (Greene *et al*., 2013), flower bud formation, fruit mass at harvest (Iwanami *et al*., 2018) and to estimate the target fruit number per tree (Handschack and Schmidt, 1990). In practice, the target fruit number per tree is, however, often estimated from the average yields of the previous years considering the mean of the entire orchard, divided by the number of trees in the orchard and the targeted fruit fresh mass. This approach leads to one level of treatment for all of the trees. This empirical method is not based on the natural variance in the capacity of each tree to support fruit of an economically desired size, namely the fruit bearing capacity (FBC), which can be highly variable within orchards (Manfrini *et al*., 2009). Therefore, the individual FBC of a certain number of trees is potentially over or underestimated by the established method. Overestimation of the FBC will lead to excessively high crop levels, poor fruit quality and reduced flower bud induction, while underestimation leads to too few fruits, a loss of crop value, reduced storability and an increased risk of storage disorders (Wójcik *et al*., 2001; Mussachi and Serra, 2018). As individual trees require a variable intensity of CLM, it is assumed that lack of tree-specific CLM is an important cause of heterogeneity in fruit size, quality, and value.

In order to observe the variability in the growth habits of trees, data from a large quantity of trees is required. Recent approaches used to detect flower clusters and the fruit of individual trees (Tsoulias *et al*., 2020) or to estimate other canopy parameters such as canopy height, volume or total leaf area, have shown promising results (Bresilla *et al*., 2019; Tsoulias *et al*., 2019; Hobart *et al*., 2020; Vanbrabant *et al.*, 2020). When these techniques are implemented within existing physiological models, the data generated can potentially be applied to estimate the photosynthetic capacity of individual trees, the optimum and target fruit number per tree, their variability within an orchard, and the required variable intensity for precise CLM practice.

The estimation of leaf area may be of outstanding importance, since the photosynthetic capacity of a tree relies on the total leaf area, especially from the exposed leaves, the quantity of light intercepted by the leaves and the photosynthetic conversion to fixed carbon. The percentage of leaf-assimilated carbohydrates partitioned to fruit, C_{part} (%), is dynamic during the whole season, with significant changes in the first weeks after bloom (Hansen, 1967; Corelli-Grappadelli *et al.*, 1994; Pallas *et al.*, 2016). The magnitude of C_{part} for a specific date is determined by the C supply to demand balance of the tree, which is influenced by the quantity and actual sink activity of all organs including shoots, fruit, leaves, branches, roots, and stem. C_{part} can range from 0% on non-bearing trees to 85% on fruiting trees with a low leaf area to fruit ratio (LA:F) (Hansen, 1969; Palmer, 1992; Lakso, unpublished data).

In periods showing C demand exceeding the supply in a particular apple tree, there is a prioritization in C partitioning among the sink organs, with the highest priority assigned to growing shoots (Bepete and Lakso, 1998). When shoot and leaf growth is complete, the highest priority for C partitioning is the fruit (Wagenmakers, 1996). When integrated over the whole season, C_{part} is defined as the harvest index (HI). For fruiting trees of different cultivars, varying HI were reported in previous studies, ranging from 50% - 85% (Koike *et al*., 1990; Palmer *et al*., 2002; Glenn, 2016; Lakso, unpublished data). They were typically grown on dwarfing rootstocks including M.9, M.26 and M.27. The HI is negatively correlated to the N supply of the tree, which positively affects the LA:F (Xia *et al*., 2009).

The C supply to the individual fruit may limit fruit growth at different times during the season (Lakso and Goffinet, 2017) and, therefore, determine the fruit size at harvest time. Hence, assuming the total leaf area per tree is closely related to light interception, the fruit size at harvest is positively correlated to LA:F (Palmer, 1992) and can be further described as a hyperbolic function of the exposed LA:F of healthy LA, not affected by external stress. The effective LA required to produce a specific fruit size from a cultivar varies depending on the exposed versus shaded LA as demonstrated by earlier studies. Hansen (1969) reviewed several early studies concerning the relationship between LA:F and fruit size, pointing out that 300-500 cm^2 LA:F, or 20-30 leaves per fruit, is the minimum requirement to achieve a marketable fruit size. The required LA:F in contemporary orchards may be different, because it may be assumed that at the time when the studies were carried out, the trees were probably not as optimally supplied with nutrients and water as in present day orchards. Other factors which affect the required LA:F are cultivar, rootstock, growing system and seasonal climate, all affecting the light interception of the trees and the HI.

Previous studies have in common that the LA:F was determined at full canopy or at harvest. However, the fruit growth rate and related C consumption of individual fruit underlies seasonal changes (Schechter *et al*., 1993; Pavel and DeJong, 1995; Lakso and Robinson, 2014). As a consequence, since seasonal leaf area and fruit development occur with different patterns, it may be assumed that the LA:F required for fulfilling the fruit's C requirement varies during fruit development. Additionally, the total LA per tree changes continuously during the season, as does the LA:F, until fruit drop and shoot growth have ended. Schumacher (1962) pointed out the negative effect of temporarily variable LA:F in order to overcome alternate bearing on Glockenapfel/M.13. The LA:F ranged from 35 -70 cm² at petal fall, 180-265 cm² before fruit drop and 530-710 cm² after fruit drop. This study indicated increasing leaf area demand per fruit to provide the C required by fruit growth during the growing period, presumably because of the increasing C requirements of the fruit and variable C assimilation by the leaves over the season. This finding was consistent with seasonal simulations applying the MaluSim carbon balance model (Lakso and Robinson, 2014). As a consequence, the FBC of the tree will be determined in phases with the highest leaf area demand per fruit, presumably in the middle of fruit development, when the fruit growth rates achieve their seasonal maximum and temperature is high.

Based on the demand and value of optimizing individual tree crop load, the objectives of the present study were (i) to quantify the fruit's daily C requirement during the growing season, (ii) to estimate the daily C assimilation of individual trees based on 2-D LiDAR measurements of the total LA, and (iii) to calculate the fruit bearing capacity of Pinova and RoHo 3615 apple trees.

MATERIAL AND METHODS

Trials were carried out in 2018 in two commercial orchards of *Malus* x *domestica* Borkh. Pinova/M.26 and RoHo 3615/M.9 (Evelina®; red mutant of Pinova) in the Brandenburg (Germany) fruit growing regions of Werder (52.357 N, 12.867 E) and Altlandsberg (52.607 N, 13.817 E) planted in 2014 and 2006, respectively. The trees were trained as tall thin central leaders with a spacing of 3.5 m × 1.25 m for Pinova and 3.2 m × 0.95 m for RoHo 3615 in Werder and Altlandsberg, respectively. The mean ground area covered by a tree was 1.15 m² in Werder and 1.05 m² in Altlandsberg. Both orchards were drip irrigated and managed according to the federal regulations of integrated production. No visible nutrient or water stress symptoms or pathogen symptoms were noted on the considered trees.

In both orchards, 45 trees were labelled and the number of flower clusters counted at green bud stage. At full bloom (Table 1) trees of RoHo 3615 were thinned with two applications of 15 kg ha^{-1} ammonium thiosulfate salt (20% N) in 500 L ha^{-1} water solution, whereas trees of Pinova were thinned with a rotating string thinner (Darwin 250, FruitTec, Markdorf, Germany) with 270 strings at 8 km h^{-1} vehicle speed and a rotational frequency of 280 rpm.

Fruit gas exchange, dry matter, elemental C content, and fruit size from randomly selected fruit, from neighbouring trees to the labelled ones, were analysed in the laboratory in two to five week intervals during the growing season. In the mid-season, when the canopies were fully developed, the total leaf area of 50 trees of Pinova and 100 trees of RoHo 3615, including the 45 labelled trees from each orchard, was estimated by means of a terrestrial mobile light detection and ranging (LiDAR) 2-D laser scanner (Tsoulias *et al*., 2019). The total yield and fruit number of the labelled trees were measured manually at 143 days after full bloom (DAFB), one day prior to commercial harvest, when randomly sampled fruit in the orchard achieved a starch index (scale ranges from 1-10) of 5.

Fruit fresh mass (FM, g), diameter (D, mm), the fraction of dry matter relative to fresh mass, DM_{rel} (0-1), and elemental C content based on fruit dry matter, C_{rel} (0-1), were measured during the entire fruit developmental period on 30 fruit per cultivar and 180 fruit per cultivar at harvest time. The samples were taken from exposed spurs in the middle of the canopy at around 2 p.m. in the afternoon. D and FM were recorded directly after sampling. During the next morning, the gas exchange of three samples, each consisting of 10 fruit until 50 DAFB (Pinova: 24 DAFB, 38 DAFB; RoHo 3615: 30 DAFB) and six samples consisting of five fruit after 50 DAFB (Pinova: 52 DAFB, 67 DAFB, 80 DAFB, 108 DAFB; RoHo 3615: 51 DAFB, 74 DAFB, 121 DAFB) were measured in the laboratory in gas-tight acrylic cuvettes, monitoring CO_2 concentration increase with continuously logging IR-CO_2 sensors (FYA600CO2, Ahlborn Mess- und Regelungstechnik GmbH, Holzkirchen, Germany). The measurements were carried out in the dark for at least two hours at 10 ± 1°C and 20 ± 1°C after the temperature adjustment of the fruit. Each of the cuvette-

Table 1. Reference dates of seasonal tree development and mean air temperature in 2 m height in two apple orchards in 2018

Cultivar	Budbreak	Full bloom	Harvest	Days from full bloom to harvest	Daily mean temperature (°C)	
	Date in 2018				0 days after full bloom (DAFB) - 45 DAFB	46 DAFB - harvest
Pinova	26.03.	04.05.	24.09.	143	19.0	19.8
RoHo 3615	22.03.	29.04.	19.09.	143	17.8	19.1

sensor systems was calibrated with technical gases (Linde, Pullach, Germany) using the concentrations 0 ppm CO_2 (N_2) and 1000 ± 20 ppm CO_2. The temperature-dependent dark respiration rate, R_{dT} (mg kg^{-1} h^{-1}), was calculated ($R_{dT} = \Delta CO_2$ (FM $\Delta t)^{-1}$), considering fruit volume, cuvette volume and actual atmospheric pressure as described earlier for the same measuring system (Brandes and Zude-Sasse, 2019). From the respiration rates obtained at two temperatures, the $Q_{10\text{-}20}$ values were calculated at each measuring date ($Q_{10\text{-}20} = R_{d20}$ R_{d10}^{-1}). For the purpose of C modelling, CO_2 was converted into C through multiplication by a factor of 0.27, resulting from the fraction of the atomic mass from C (12.01 g mol^{-1}) on the molar mass of CO_2 (44.01 g mol^{-1}).

Afterwards, 10 fruit (< 50 DAFB), 5 × 0.5 fruit (> 50 DAFB) per measurement were dried at 80°C until a constant mass was reached. DM_{rel} was calculated by dividing the mass of the dry matter by the initial FM of the sample before drying. The dry matter was homogenized with a mixer mill (MM400, Retsch Technology, Haan, Germany) at a frequency of 30 Hz for 1 min. C_{rel} of the homogenized dry matter was measured with an elemental analyser (Vario EL III, Elementar Analysensysteme GmbH, Hanau, Germany) at 1150°C. The absolute C content per fruit (C_{fruit}, g), was then calculated (C_{fruit} = FM DM_{rel} C_{rel}).

After the canopy of the trees was fully developed, usually in mid-July, individual trees (Altlandsberg: 81 DAFB, n = 100; Werder: 67 DAFB, n = 50) were scanned with a 2-D LiDAR laser scanner (LMS511 pro model, Sick, Düsseldorf, Germany) with an angular resolution of 0.1667° and a scanning frequency of 25 Hz at a vertical scanning angle of 270°. The LiDAR laser scanner was placed together with an inertial measurement unit (MTi-G-710, XSENS, Enschede, The Netherlands) and a RTK-GNSS (AgGPS 542, Trimble, Sunnyvale, CA, USA) on a metal platform at a height of 1.6 m (Tsoulias *et al*., 2019). The platform was mounted on a tractor and driven along each side of the tree rows with an average speed of 0.13 m s^{-1} to acquire the 3-D point cloud of each tree. The LiDAR points were filtered considering only the observations between a height of 0.05 m and 4.00 m, while the points that belonged to the ground were removed utilizing the random sample consensus algorithm. Thus, the LiDAR points per tree (PPT) were extracted from the 3-D point cloud with an own Matlab script (Version 2016b, The Mathworks Inc., Natick, MA, USA) (Tsoulias *et al*., 2019). In order to calibrate PPT on the total LA per tree, LA_{LiDAR} (m²), six trees per orchard were defoliated and the total LA, LA_{lab} (m²), was measured in the laboratory. All leaves per tree were sorted by size into three fractions (small, medium, large). The number of leaves in each fraction was counted. The average leaf size per fraction was analysed from manual scans of 20% of the leaves, from each fraction, with a desktop scanner (Scanjet 4850, HP, Palo Alto, CA, USA), in groups of 5-15 leaves. The RGB-images were analysed considering the sum of pixels of each leaf, with own Matlab script. An area of 6241 pixels in the image equalled an area of 1 cm². The number of pixels per leaf was converted into cm² leaf area per leaf by division with the factor 6241.The average leaf size per fraction was multiplied by the number of leaves per fraction. LA_{lab} is the sum of the leaf area from each leaf fraction. Regression analysis between PPT and LA_{lab} was carried out with software R (Version 3.4.1; R Core Team, 2018). The regression models between PPT and LA_{lab} were used to convert the individual PPT of individual trees scanned in the orchards into LA_{LiDAR}. The coefficient of determination, R^2, and the relative root mean squared error, RRMSE (%) were calculated considering LA_{LiDAR} and LA_{lab} (Eqs A1, A2).

The seasonal development of the total leaf area of individual trees, LA_{tree} (m²), was estimated by fitting $^{mean}LA_{LiDAR}$ of both cultivars into a sigmoid growth model based on the number of days after bud break (DABB) (Eq. A3) with Table Curve 2D (Version 5.01, IBM Corporation, Armonk, NY, USA). It was assumed that LA_{tree} was 0 at bud break (Table 1), 20% of $^{mean}LA_{LiDAR}$ at full bloom (cf. Lakso *et al*., 1984; Wünsche *et al*., 1996). In an earlier study, it was reported that the canopy of apple trees, grown on a dwarfing rootstock, was fully developed after 1200 accumulated growing degree d on base temperature (T_B, °C), of 4°C, $GDD_{4°C}$ (Eq. A4), after bud break (Doerflinger *et al*., 2015). In the current study 1200 $GDD_{4°C}$ were achieved at 07.07.2018, 13.07.2018 for Pinova and RoHo 3615, respectively. After those dates LA_{tree} was assumed to remain constant until harvest. T_{max} and T_{min} are the daily minima and maxima of T in 2 m height in the orchards.

The maximum quantum yield, $^{max}\alpha$ (mol mol^{-1}), and the light saturated net CO_2 gas exchange rate, $^{max}J_{CO_2}$ (µmol m^{-2} s^{-1}), were derived from the light response curves of the net CO_2 gas exchange rates, J_{CO_2} (µmol m^{-2} s^{-1}), measured on three mature leaves of RoHo 3615 in exposed positions of the canopy of bearing trees on seven dates during fruit development (DAFB: 7, 27, 32, 66, 71, 92, 108). Measurements were carried out using a portable porometer (LI-6400 XT, LI-COR Inc., Lincoln, NE, USA) coupled with a broadleaf cuvette equipped with a red and blue LED light source (6400-40, LI-COR Inc., Lincoln, NE, USA). An area of 1.7 cm² per leaf was fixed inside the cuvette for the measurements. The measurements were performed at ambient leaf temperature, T_{leaf}, and relative humidity at a constant CO_2 mole fraction of 400 µmol mol^{-1} in the reference gas flow and a range of photosynthetic photon flux rates, PPFR (µmol m^{-2} s^{-1}), (2,000; 1,500; 1,000; 750, 500, 250, 110, 50, 20, 0) with waiting times between 80 and 120 s. $^{max}\alpha$ was calculated as the initial slope of J_{CO2} *vs*. PPFR between 0 and 110 µmol m^{-2} s^{-1} , whereas $^{max}J_{CO_2}$ was considered to be equivalent to J_{CO_2} at 2000 µmol m^{-2} s^{-1}.

The means of FM and C_{fruit} were interpolated over the season and expressed as sigmoid functions of DAFB (Eqs A5, A6). The first derivatives of the equations were calculated and referred to as absolute growth rates considering

FM, AGR_{FM} (g d^{-1}) and C, AGR_C (g d^{-1}), (Eqs A7, A8). The daily elemental C requirements to account for the observed growth and respiration per fruit (C_{daily}, g d^{-1}), is the sum of AGR_C and the daily respired C per fruit (R_{daily}, g d^{-1}) ($C_{daily} = AGR_C + R_{daily}$). R_{daily} (C, g d^{-1}) was calculated (Eq. (1)) from the estimated respiration rate of the fruit in the field (R_{field}, mg kg^{-1} h^{-1}), multiplied by the daily interpolated values of FM between the sampling dates, with the simplifying assumption that no diurnal changes in R_{dT} occurred.

$$R_{daily} = \frac{R_{field}\ FM\ 24}{1000}\ 0.27, \tag{1}$$

R_{field} (CO_2, mg kg^{-1} h^{-1}) was estimated (Eq. (2)) from R_{d10} and R_{d20} measured in the laboratory, and the average daily temperature (T_{mean}, °C), in the same orchard in Altlandsberg and a neighbouring orchard in Werder (52.453684 N, 12.824633 E), recorded in 2 m height with a PT100 temperature sensor (Pessl Instruments GmbH, Weiz, Austria).

$$R_{field} = R_{d10} + \frac{(T_{mean} - 10°C) \times (R_{d20} - R_{d10})}{10°C}. \tag{2}$$

To estimate C_{daily} for varying fruit size at harvest time (D = 65, 70, 75, 80 mm) the equations A5 and A6 were normalized for FM and C at harvest time (143 DAFB). The normalized functions (Eqs A9, A10) were used to fit growth curves for the targeted fruit sizes (Fig. A1b) and the associated daily growth rates, AGR_{FM} and AGR_C. C_{daily} was calculated from these growth curves under the assumption that the respiration rate per fresh mass unit (R_{field}) was identical for all fruit sizes.

The necessary LA required to assimilate C_{daily}, LA_{demand} (cm^2), was calculated (Eq. (3)) from the daily assimilated C per unit ground area (P_{daily}, g m^{-2} d^{-1}), and the percentage of assimilated carbohydrates partitioned to fruit (C_{part}, %). LA_{demand} was calculated for variable amounts of C_{part}. A linear increase in C_{part} from 40% at full bloom to 80%, when the foliage was fully developed was assumed (cf. Wagenmakers, 1996). It was also assumed that fruit photosynthesis contributes 5% of the fruit's carbon demand. To reduce the effect of local maxima of LA_{demand}, originating from days with low solar radiation (Eq. (4)), the seasonal course of LA_{demand} was smoothed with a Savitzky-Golay filter, using the R-Package signal (Ligges *et al*., 2015; sgolayfilt, filter order = 1, filter length = 9).

$$LA_{demand} = \frac{0.95\ C_{daily}}{\left(\frac{P_{daily}\ C_{part}}{LAI_{orchard}\ 10000}\right)} \tag{3}$$

P_{daily} (C, g m^{-2} d^{-1}) was calculated (Eq. (4)) according to the equation of the canopy daily net photosynthesis integral of Charles-Edwards (1982), adapted to apple (Lakso and Johnson, 1990; Lakso *et al*., 2001, 2006):

$$P_{daily} = \frac{^{max}\alpha\ S\ DL\ ^{max}J_{CO2}\ P_T\ LI}{^{max}\alpha\ k\ S + h\ ^{max}J_{CO2}\ P_T}\ 0.27, \tag{4}$$

$$LI\,[0\text{-}1] = F_{max}\ (1 - e^{(-k\ \frac{LAI_{orchard}}{F_{max}})}), \tag{5}$$

$$P_T\,[0\text{-}1] = 0.535 + 0.0384\ T_{day} - 0.0004126\ T_{day}^2 - 0.00001576\ T_{day}^3. \tag{6}$$

For the purpose of the model, the seasonal mean values of $^{max}\alpha$ and $^{max}J_{CO_2}$ (0.054 mol mol^{-1}; 17.2 µmol m^{-2} s^{-1}) were converted into 5.43 µg J^{-1} and 0.000758 g m^{-2} s^{-1}, respectively, assuming that the fraction of the photosynthetic active radiation, PAR, from the total radiation was 0.5 and the conversion factor from µmol s^{-1} m^{-2} (PAR) to W m^2 (PAR) was 0.2188 (McCree, 1972). The daily integral of solar radiation, S (MJ m^{-2} d^{-1}), was recorded by a pyranometer (CMP 3, Kipp & Zonen, Delft, The Netherlands) in the spectral range of 300-2800 nm. The day length, DL (s), resulted from the daily hours, with solar radiation > 0 W m^{-2} h^{-1}, multiplied by 3600 s h^{-1}. LI (Eq. (5)) is the fraction of light intercepted by the canopy (cf. Jackson and Palmer, 1980). The canopy's light extinction coefficient (k), and the fraction of total radiation actually incident to the canopy, F_{max}, were assumed to be 0.5 and 0.7, respectively (Lakso *et al*., 2006). An F_{max} of 0.7 assumes that 30% of the incident radiation is lost to the ground regardless of the tree's leaf area. Daily values of LAI of the whole orchard, $LAI_{orchard}$, were calculated from the ground area allotted per tree ($G_{allotted}$, m^2), divided by the daily value of LA_{tree}. $G_{allotted}$ is determined by the spacing between the trees and rows, and was 4.375 and 3.040 m^2 for Pinova and RoHo 3615, respectively.

The relative effect of temperature on P_{daily}, P_T [0-1], was included (Eq. (6)), taking into account the average temperature during the daylight period (T_{day}, °C). The normalised equation of P_T was estimated from several studies at Cornell AgriTech (cf. Lakso *et al*., 1999). The daily amount of assimilated C per tree, P_{tree} (g d^{-1}), and the fruit bearing capacities (FBC, fruit $tree^{-1}$) of the trees for several target fruit sizes, FBC, were calculated (Eqs (7), (8)).

$$P_{tree} = P_{daily}\ G_{allotted}, \tag{7}$$

$$FBC = \frac{LA_{tree}}{LA_{demand}}. \tag{8}$$

RESULTS

A sigmoidal growth model was applied to interpolate the measured values of fresh mass and C as a function of time (Fig. 1a, 1e), because the linear interpolation of individual means led to an unrealistic fluctuation in growth rates, which was most likely a consequence of the sampling of random fruit at each date. The model was in good agreement with the measured values (Pinova: $R^2 = 0.85$; RoHo 3615: $R^2 = 0.87$). A high degree of deviation was found in RoHo 3615, at 100 DAFB which would have resulted in very high growth rates > 2.5 g d^{-1} (AGR_{FM}), more than double that of the neighbouring values. Since the weather data in both periods did not indicate strong changes or extreme weather events and the water supply to the trees was unchanged, this variation wasn't taken into account in the subsequent analysis. Fruit of Pinova developed elevated growth rates (AGR_C, AGR_{FM}) in comparison to RoHo 3615 from 22 DAFB to 100 DAFB (Figs 1b, 1f), although the average temperatures in the cell division stage was similar in both orchards (Table 1). Both growth rates of Pinova peaked 9 days earlier compared to RoHo 3615. The result was that the average fresh mass (FM) and absolute C content of Pinova fruit exceeded that of RoHo 3615 at harvest time.

The dry matter content (DM_{rel}) and C content of dry matter (C_{rel}) of fruit from both cultivars followed similar seasonal courses (Fig. 1c, 1d). While DM_{rel} showed slight seasonal fluctuations, C_{rel} decreased linearly within the range from 0.51 to 0.47 (Eqs A11).

The dark respiration rates per unit of fresh mass of both cultivars decreased during fruit development in a typical course for apple (Jones, 1981), but at 10°C to a lower extent than at 20°C (Fig. 2a). At 38 DAFB and 52 DAFB, the R_{d20} value of Pinova fruit was elevated in comparison to the fruit of RoHo 3615. The Q_{10-20} values indicated that an increase in temperature from 10 to 20°C resulted in a 1.4-4.0 fold increase in R_{dT} (Fig. 2b). As a consequence of elevated FM and R_{field}, the R_{daily} of Pinova was enhanced until 65 DAFB in comparison to RoHo 3615. Accordingly, the total of respired C per fruit from 30 DAFB until harvest (114 d) was higher on Pinova (1.67 g) in comparison to RoHo 3615 (1.33 g), accounting for 10.4 and 10%, respectively, of the accumulated daily C requirement per fruit. The daily fluctuation in the percentage of respiration of C_{daily} ranged from 6-44%. Hence, C_{daily} was mainly determined by C accumulation, AGR_C, which is reflected in a similar seasonal course. In total, fruit of RoHo 3615 consumed 13.3 g of C in the period from 30 DAFB till harvest, achieving an average FM of 165 g, whereas Pinova fruit

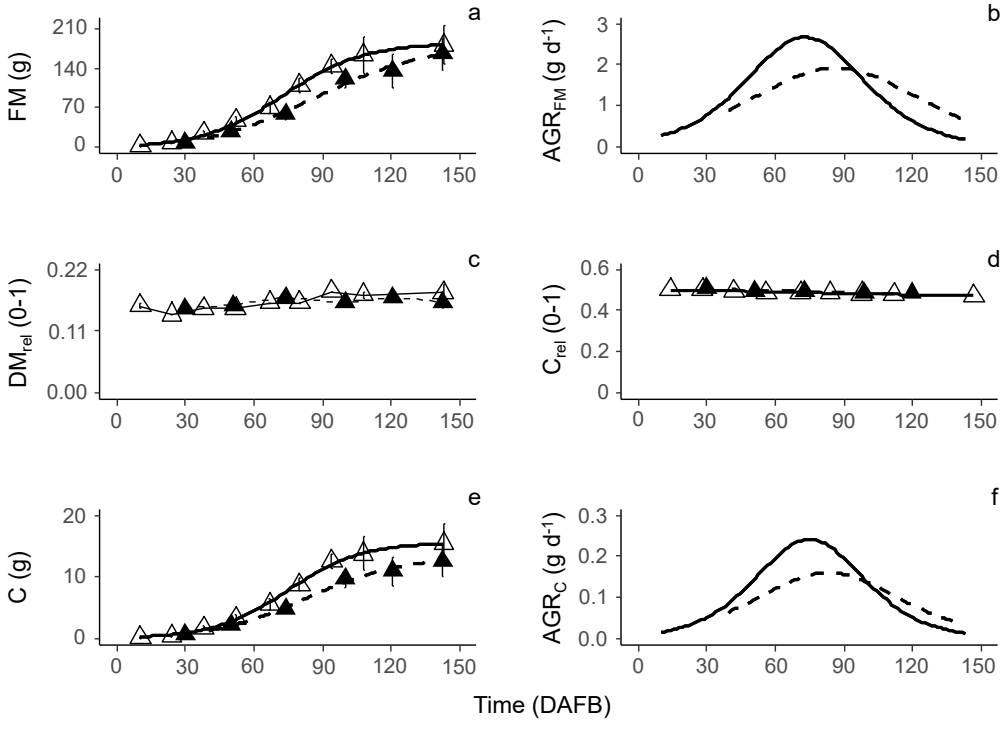

Fig. 1. Time course in days after full bloom (DAFB) of (a) fresh mass (FM, g), (b) absolute growth rate of fresh mass (AGR_{FM}, g d^{-1}), (c) fraction of dry matter (DM_{rel}) on FM (0-1), (d) fraction of elemental C on DM_{rel} (0-1) (C_{rel}), (e) absolute C content (g), (f) absolute growth rate in C (AGR_C, g d^{-1}) of developing Pinova/M.26 (open symbol, solid line) and RoHo 3615/M.9 (closed symbol, dashed line) apple fruit during the 2018 growing season. Error bars indicate the standard deviations.

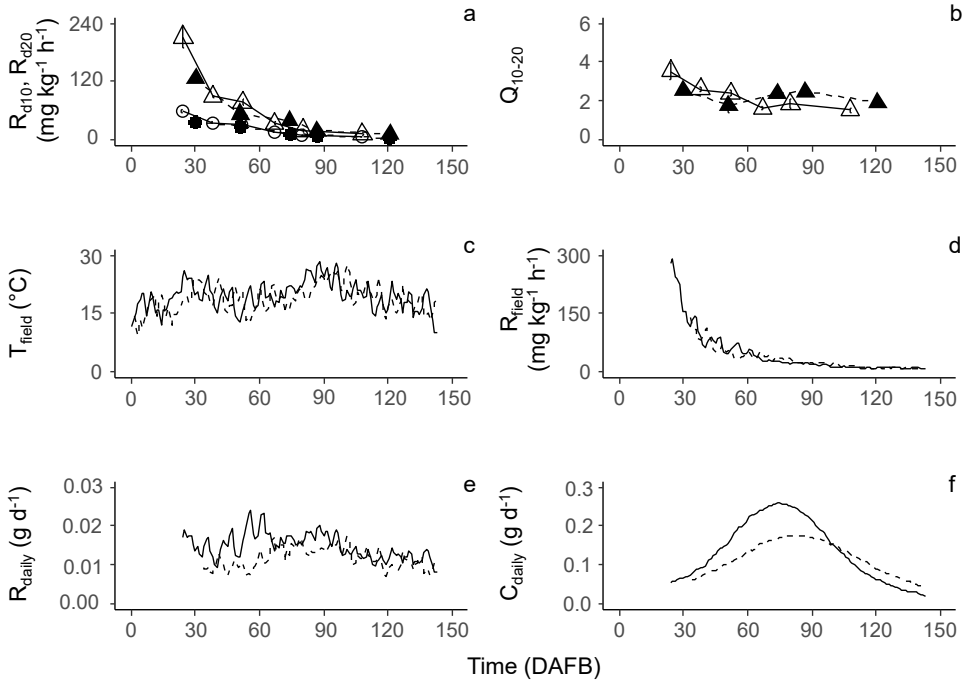

Fig. 2. Time course in days after full bloom (DAFB) of: a) fruit CO_2 respiration rate (mg kg^{-1} h^{-1}) at 10°C (R_{d10}, circle) and 20°C (R_{d20}, triangle); b) Q10-20 values for fruit respiration between 10 and 20°C; c) mean daily temperature (T_{mean}, °C) at a height of 2 m; d) estimated respiration rates (R_{field}, mg kg^{-1} h^{-1}) calculated for T_{mean}; e) daily respired C per fruit (g d^{-1}); f) daily C requirement per fruit (g d^{-1}) of Pinova/M.26 (open symbol, solid line) and RoHo 3615/M.9 (closed symbol, dashed line) apple fruit during the 2018 growing season. Error bars indicate the standard deviations.

consumed 16.1 g of C in the same period, achieving 182 g FM. When estimated for varying target fruit size, C_{daily} rose up to maximum of 0.35 g d^{-1} in Pinova fruit (Fig. 3a), while the targeted fruit size was 80 mm, which equates to 244 g FM at harvest (Fig. A1).

The total leaf area per tree measured in the laboratory, LA_{lab}, and LiDAR points per tree, PPT, were highly correlated in both orchards (Fig. 4). Although the relationship would be expected to be hyperbolic, within the abundant range of leaf area, linear models between PPT and LA_{lab} were adequate to estimate LA_{LiDAR} from the PPT of all scanned trees (Eqs A12.1, A12.2). The RRMSE between the measured and estimated leaf area per tree was 3.8 and 3.0% for Pinova and RoHo 3615, respectively.

LA_{LiDAR} of Pinova trees was on average 3.8 ± 0.55 m² (10.07.2018) showing a wide range of 2.5 m² - 4.9 m², whereas LA_{LiDAR} of RoHo 3615 was 5.3 ± 0.95 m² (19.07.2018) (Fig. 4) with a total range of 3.3 m² - 7.6 m². The resulting $^{mean}LAI_{orchard}$ was 0.87, 1.75, on Pinova, RoHo 3615, respectively. The assumed development of the leaf area per tree from bud break till harvest was estimated (Fig. 5) by fitting $^{mean}LA_{LiDAR}$ into a sigmoidal growth model (Eqs A13.1, A13.2).

The average maximum quantum yield of the leaves, $^{max}\alpha$, (Fig. 6) over the entire season of RoHo 3615 was 0.054 ± 0.003 mol mol^{-1}. The light saturated net CO_2 gas exchange at ambient temperature, in comparison, showed

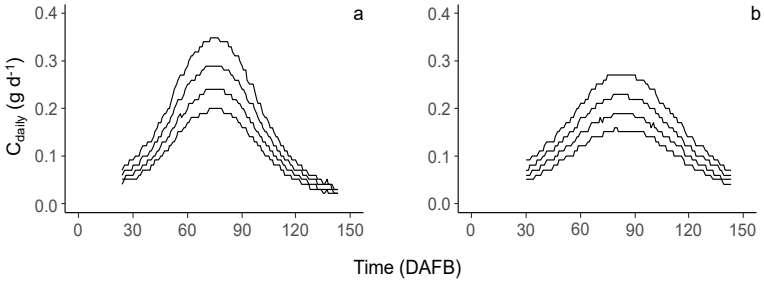

Fig. 3. Time course in days after full bloom (DAFB) of daily C requirement per fruit (g d^{-1}) considering (a) Pinova/M.26 and (b) RoHo 3615/M.9 apple fruit with varying target fruit sizes (from the bottom up: 65, 70, 75, and 80 mm) estimated for the conditions in the considered orchards in 2018.

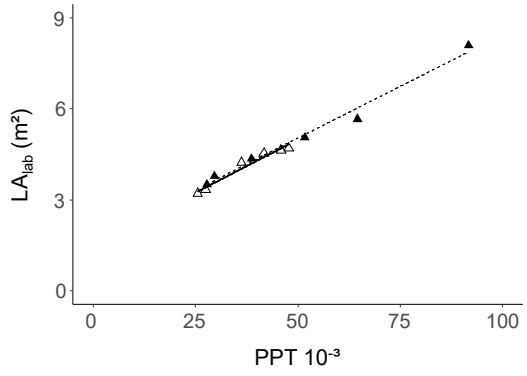

Fig. 4. Relationships between laser hits per tree (PPT) and manual measured total leaf area per tree (LA_{lab}, m²). (RoHo3615: closed symbol, dotted line; LA_{lab} = 1.6 + (6.822 10^{-5} PPT), R^2 = 0.98; Pinova: open symbol, solid line; LA_{lab} = 1.49 + (6.987 10^{-5} PPT, R^2 = 0.96.

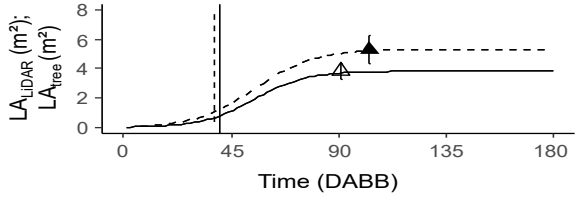

Fig. 5. Estimated seasonal course in days after bud break (DABB) of total leaf area per tree (LA_{tree}, m²) and LiDAR estimated LA (LA_{LiDAR}, m²) of Pinova/M.26 (open symbol, solid line) and RoHo 3615/M.9 (closed symbol, dashed line) in 2018. Vertical lines indicate the date of full bloom, error bars the standard deviation.

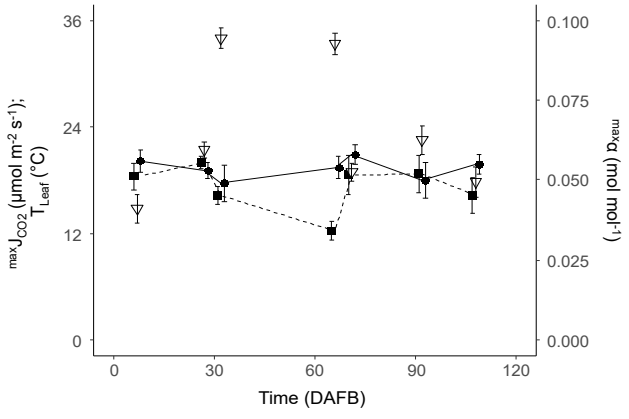

Fig. 6. Seasonal course (days after full bloom (DAFB)) of the maximum quantum yield ($^{max}\alpha$, mol mol^{-1}) (filled circle, solid line), light saturated CO_2 leaf gas exchange ($^{max}J_{CO_2}$, µmol m^{-2} s^{-1}), (filled square, dashed line), and leaf temperature (T_{leaf}, °C) (open triangle) during the leaf gas exchange measurements of developing RoHo 3615/M.9 apple leaves during the 2018 growing season. Error bars indicate the standard deviations.

Table 2. Leaf area per tree, associated percentage of light intercepted and mean daily carbon assimilation per tree ($^{mean}P_{tree}$) of Pinova/M.26 and RoHo 3615/M.9 apple trees in the 2018 growing season after the foliage of the trees was fully developed

Cultivar/ Spacing	LA_{tree} (m²)	Light interception* (%)	$^{mean}P_{tree}$ (C; g tree^{-1} d^{-1})
Pinova/ 3.5 m × 1.25 m	2.5	23	10.9*
	3.8	32	15*
	4.9	39	17.9*
RoHo 3615/ 3.2 m × 0.95 m	3.3	38	11.9**
	5.3	50	15.6**
	7.6	58	18.3**

In the period: *from 66 days after full bloom (DAFB) until harvest, 143 DAFB **76 DAFB until harvest, 143 DAFB.

higher seasonal fluctuations, as a response to varying leaf temperature and vapour pressure deficit (data not shown) at the different measurement dates.

The percentage of light intercepted by the canopy and the average daily assimilated C per tree, when the foliage was fully developed until harvest, was elevated on RoHo 3615 in comparison to Pinova (Table 2, Fig. 7). The difference resulted from the higher leaf area per tree of RoHo 3615 in combination with the reduced distances between trees and rows. Seasonal variation in P_{tree} occurred, reflecting the seasonal course in solar radiation (Fig. 7). The daily leaf area demand per fruit, LA_{demand}, showed a high degree of fluctuation during the growing season on both cultivars and appeared to be inverse to the seasonal course of S. On 12.07.2018, LA_{demand} reached its height, due to the local minima in S (Altlandsberg: 4.2 MJ m^{-2} d^{-1}; Werder: 7.1 MJ m^{-2} d^{-1}). Local minima and maxima were smoothed with a Savitzky-Golay filter without affecting the seasonal means in LA_{demand}. When dividing the seasonal course of LA_{demand} in 30 day intervals, the means of the original and the smoothed values of LA_{demand} for each interval differed by a maximum 3 cm² (data not shown). During whole fruit development LA_{demand} conformed to AGR_C and appeared to reach its highest points when AGR_C reached its highest values in the middle of the growing period (Fig. 1f, 3, 7e, 7f).

The mean LA_{demand} considering varying fruit size in the period of 30 days after the foliage was fully developed (Pinova: 66 DAFB - 95 DAFB, RoHo 3615: 76 DAFB – 105 DAFB) increased with targeted fruit size (Fig. 8). The estimations, additionally demonstrated that the LA_{demand} to produce a target fruit size at harvest increases with total leaf area per tree (Fig. 8), as a consequence of increasing the internal shading of the leaves and the associated decrease in available light per leaf. Models used to estimate LA_{demand} for fruit of varying sizes on trees with a range in LA_{tree} of the observed trees were developed (Eqs 9.1, 9.2), based on the values plotted in Fig. 8. The average individual leaf

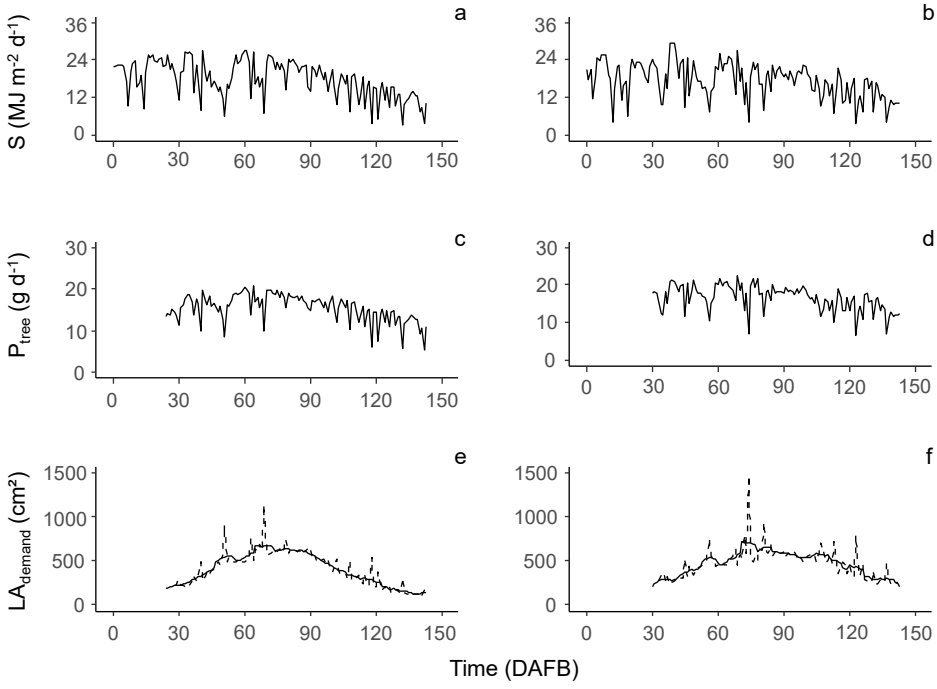

Fig. 7. Time course in days after full bloom (DAFB) of (a, b) solar radiation (S, MJ m^{-2} d^{-1}) and (c, d) estimated daily C assimilation per tree (P_{tree}, g d^{-1}) (e, f) daily leaf area demand per fruit (LA_{demand}, cm²) (percentage of leaf-assimilated C available for fruit: linear increase from 40% (full bloom) to 80% (foliage is fully developed and the period of time after that)) of developing Pinova/M.26 (a, c) and RoHo 3615/M.9 (b, d) apple during the 2018 growing season. The fruit mass and size at harvest time were (e) 182 g / 72 mm, (f) 165 g / 68 mm. (e, f): solid line = smoothed values, dashed line = original values).

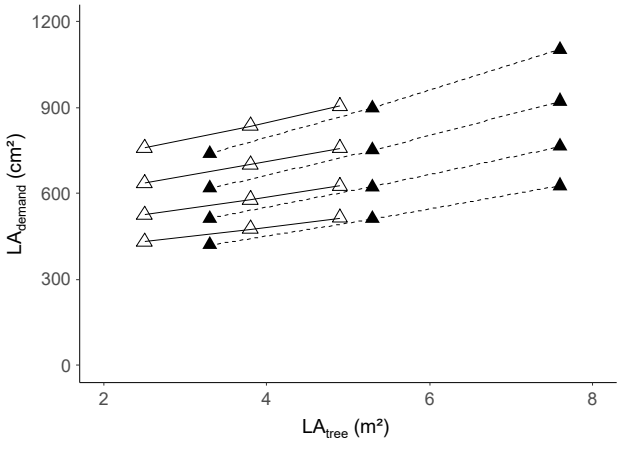

Fig. 8. Leaf area demand* (LA_{demand}, cm²) per fruit of Pinova/M.26 (open symbol, solid line) and RoHo 3615/M.9 (closed symbol, dashed line) apple with varying harvest fruit size (bottom to top: 65, 70, 75, and 80 mm) for trees with a different total leaf area (LA_{tree}, m²) (* mean values in the period of 30 days after foliage was fully developed, Pinova: 66 d after full bloom – 95 DAFB, RoHo 3615: 76 DAFB – 105 DAFB in 2018).

area, considering leaves from spurs and extension shoots in both orchards, was 24 cm² (data not shown). The resulting leaf demand per fruit would range from 18 – 38 leaves per fruit for Pinova and 18 – 46 leaves per fruit for RoHo 3615 for the targeted fruit sizes and a given total leaf area per tree in both orchards. Model equations 9.1 and 9.2 were used to calculate the individual fruit bearing capacity (FBC) of trees with the varying total leaf area (Fig. 9). The difference in FBC between the trees in the range of the measured leaf area per tree is considerable. The FBC for a targeted fruit diameter of 65 mm for trees with a high total leaf area exceeds that of trees with a low leaf area by 50%. Both cultivars are known for their low susceptibility to alternate bearing and, therefore, alternate bearing was not considered in the present study. It may also be assumed that at the crop level equal to the FBC, alternate bearing is not expected.

$$\text{Pinova: } LA_{demand}(D, LA_{tree}) = -795.12 + 17.44\,D - 79.95\,LA_{tree} + 1.76\,D\,LA_{tree} \quad (9.1)$$

$$\text{RoHo 3615: } LA_{demand}(D, LA_{tree}) = -598 + 13.12\,D - 110.9\,LA_{tree} + 2.44\,D\,LA_{tree} \quad (9.2)$$

LA_{demand} was estimated using Eqs (9.1), (9.2) taking into account the average fruit size per tree at harvest and the measured LA_{tree} of the individual trees. The LA_{demand} was applied to calculate the FBC of individual trees to produce fruit of the abundant average fruit size. LA_{demand} was compared to the actual LA:F of individual trees, whereas FBC was validated with the number of fruit per tree of the same trees at harvest (Fig. 10). The results demonstrate that the

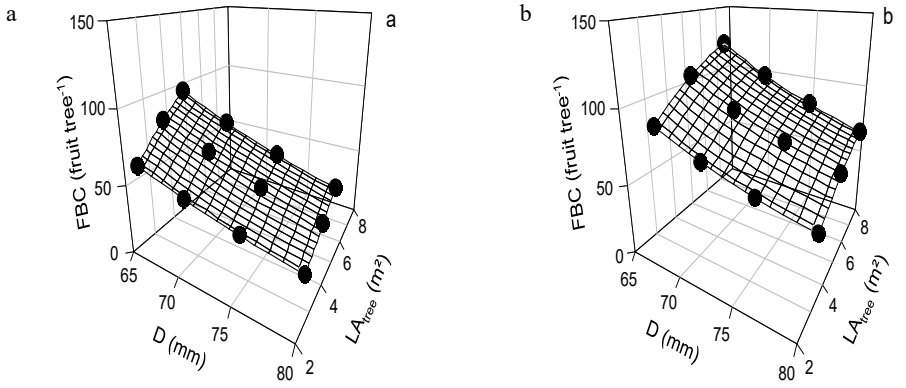

Fig. 9. Fruit bearing capacity (FBC, fruit tree^{-1}) considering trees with a varying canopy leaf area (m²), when the canopy is fully developed, of Pinova (a) and RoHo 3615 (b) in 2018 to produce fruit of a certain target fruit diameter (D, mm). The closed dots represent min, mean and max values of LA_{tree} in the considered orchards, cf. Table 2.

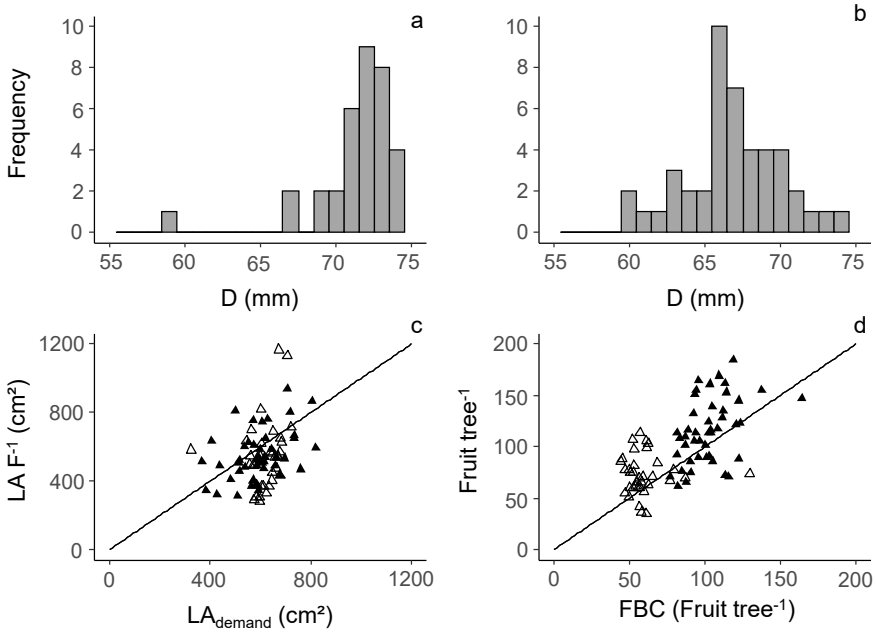

Fig. 10. a, b) Distribution of the average fruit diameter* (mm) of individual apple trees; c) comparison between the modelled LA_{demand} (cm²) to achieve the average fruit diameter and the measured leaf area to fruit ratio (LA F^{-1}, cm²); d) estimated fruit bearing capacity (FBC)**, to achieve measured average fruit diameter and harvested fruit per tree of Pinova (a, n = 35; open symbol) and RoHo 361 (b, n = 45; closed symbol) in 2018. Solid lines represent (c) LA:F = LA demand (d) FBC = harvested fruit per tree (* the average fruit diameter was derived from the average fresh mass as shown in Fig. A1; ** in the period 30 days after the tree canopy was fully developed).

mean fruit number per tree in both cultivars was close to the calculated FBC. However, 8 trees out of 35 trees of Pinova and 14 trees out of 45 trees of RoHo 3615 had an LA:F value which was too high, thereby exceeding LA_{demand} by an average of 208 cm² and 126 cm², respectively (Fig. 10). Consequently, when comparing fruit per tree and FBC, it should be noted that 23% of the Pinova trees and 31% of RoHo 3615 trees had too few fruit per tree below the FBC. The average fruit fresh mass from the latter trees was 165 g, 159 g for Pinova and RoHo 3615, respectively.

When scaled up to the whole orchard level, Pinova could bear 1.9 t ha^{-1}, RoHo 3615 3.1 t ha^{-1} more fruit, which equates to 6 and 5% of the current yield of the orchards of 29.8 and 59.6 t ha^{-1}, respectively. Consequently, the data show that a substantial number of trees are not managed at their optimal FBC. The number of flower clusters per tree in 2018 exceeded the FBC (data not shown) and no late frost reduced the number of fruit per tree in both orchards. The field uniform flower thinning may be seen as the primary source for the reduction in fruit per tree below the FBC.

In contrast, 16% of the trees of RoHo 3615 bore too many fruit per tree, exceeding the FBC by an average of 19 fruits per tree, leading to a low average fruit size below 65 mm (Fig. 10b), which is the minimum requirement for fresh market entry. As a consequence, despite high yields, the crop value from the mentioned trees is reduced.

DISCUSSION

The purpose of this study was to investigate seasonal fruit growth and the variability in growth and fruit bearing capacity of individual trees within commercial apple orchards. Previous studies demonstrated the variability in yield and fruit per tree within orchards (Manfrini *et al*., 2009; Aggelopoulou *et al*., 2010), which is proposed to be considered in orchard management instead of the uniform treatment of all trees. The photosynthetic capacity of the trees and the associated light interception, which is a major determinant of crop growth (Monteith, 1977), was, however, not investigated. To further advance precise crop load management and adapt it to the site specific conditions, knowledge concerning the daily and seasonal carbon fixation of individual trees and the carbon requirements of developing fruit is required, this allows for the optimization of the carbon supply to demand balance of the tree to produce a desired fruit size. Existing carbon balance models (Lakso *et al*., 2006; Pallas *et al*., 2016) could adequately express the carbon supply to demand balance of individual apple trees and estimate the resulting number of fruit per tree and their fruit fresh mass at harvest for the conditions of individual seasons as well as the influence of different management practices on them. However, as one major input factor is the quantity of shoots per tree of different shoot populations, to generate leaf areas, it would be time consuming to count them from a high quantity of trees within an orchard for this purpose. The application of LiDAR in horticulture enables the quantification of canopy parameters, such as the total leaf area per tree, georeferenced for all trees of an orchard (Arno *et al*., 2012; Tsoulias *et al*., 2019; Hobart *et al*., 2020). When integrated into the existing carbon balance models or parts of it, these plant data can provide an overview of the variability in carbon fixation per tree and the potential crop growth of whole orchards, for possible application in precision tree-specific crop load management.

A seasonal dynamic in carbon demand per fruit was demonstrated in the presented study, depending on the different development stages and associated sink strength per fruit as determined by the number of cortical cells (Lakso and Goffinet, 2017). The seasonal development of apple fruit from full bloom until harvest may be divided into two main stages, that overlap somewhat: cell division and cell enlargement, both with characteristic growth habits (Schechter *et al*., 1993). However, there is a smooth transition between the stages as cell division in the cortex ends around 40-45 DAFB, whereas it continues in the epidermis until 70 DAFB or even longer (Schechter *et al*., 1993; Skene, 1966). Early fruit growth in fresh mass under the non-limiting conditions of low crop and no environmental stress follows a curvilinear course until about five weeks after full bloom before transitioning into a linear increase (Lakso *et al*., 1995). A gradual decrease in the growth rate in the last part of the fruit development phase until the final fruit size is achieved is often seen but may reflect a reduced carbon supply or limiting temperatures or radiation (Stanley *et al*., 2000). Despite the absence of data in the first weeks of fruit growth in the present study, the seasonal growth of fruit from both cultivars followed a course with typical peaks in growth rates in the middle of fruit development (Stanley *et al*., 2000).

The maximum growth rates of the fruit in the present trials, modelled for different target fruit sizes, were within the range of growth rates in FM of Delicious apple, as reported previously, with a final fruit mass of between 165 g and 260 g (Warrington *et al*., 1999) and Royal Gala apple with a final fruit mass of 200 g (Stanley *et al*., 2000). The dry matter content of the fruit was, in comparison to earlier findings (Schechter *et al*., 1993), relatively stable without noticeable changes occurring between the development stages. Minor fluctuations possibly occurred as a consequence of water flows inside and outside the fruit. The C content of the dry matter appeared to be slightly elevated in comparison with earlier results (Walton *et al*., 1999). However, a decrease in C_{rel} from bloom until harvest was also observed, which occurs hypothetically due to changes in the composition of dry matter during fruit development with the accumulation of primarily carbohydrates that consist of approx. 40% C (Pavel and DeJong, 1995).

Dark respiration, generally, provides the chemical energy (*i.e.* ATP) necessary for the maintenance and growth processes in cells. During cell division, relatively more nucleic acids and proteins are formed in comparison to cell enlargement, which involves the vacuoles of the cells being filled with carbohydrates and organic acids for the most part (Walton *et al*., 1999). Therefore, the respiration rate per unit fresh mass is higher in the cell division period than in the cell enlargement period which is more of a storage process. This leads to the typical seasonal decrease in the fruit respiration rate per unit fresh mass until cortex cell division ends. Afterwards, the respiration rate remains relatively constant (Figs 2a, 2d) until the climacteric rise. The fruit in the present trial, however, was harvested before the climacteric rise in fruit respiration rate occurred.

The seasonal decrease in $Q_{10\text{-}20}$ (Fig. 2b) observed for both cultivars, was also reported previously for the $Q_{15\text{-}25}$ values of the Golden Delicious apple, decreasing from 2.8 in early June to 1.6 in early August (Jones, 1981). The daily integral of respired CO_2 by an apple (R_{daily}) is determined by R_{dT}, fresh mass and temperature, which all change continuously. Consequently, R_{daily} fluctuated significant during

the whole fruit development process (Fig. 2e). As a result of elevated R_{dT} and FM, R_{daily} was higher on Pinova in comparison to RoHo 3615, especially in the period until 67 DAFB (Fig. 2e). Diurnal changes in fruit respiration, independent of fruit temperature, as described earlier (Bepete and Lakso, 1997), were not considered for the current calculations.

Apart from the aforementioned factors, the daily magnitude of fruit growth and respiration, in general, depends on the amount of carbohydrates translocated to the fruit, mainly in the form of sorbitol and sucrose (Hansen, 1967). Because approximately 90% of the annual carbohydrates assimilated by a tree are assimilated in the leaves (Hansen, 1967), the leaf area per fruit ratio, LA:F, and the available light limit fruit growth.

Both the leaf area demand after the canopy was fully developed and the fruit fresh mass were within the normal range of the results described for cultivars with medium size fruit grown on dwarfing rootstocks (cf. Palmer, 1992; Xia *et al*., 2009). Larger fruit sizes at enhanced leaf area to fruit ratios were reported for the cultivars Braeburn (Palmer *et al.*, 1997) and Fuji (Koike *et al*., 1990), where the genetic predisposition enables growth to a fresh mass exceeding 320 g at LA:F > 1200 cm².

The daily amount of fixed carbon per tree depends on the amount of intercepted light by the canopy, which also limits its annual yield. The relationship between the fraction of intercepted light by a canopy and the leaf area index of a tree may be described as a hyperbolic function (Eq. (6)). A similar hyperbolic function was expected for the calibration model concerning LiDAR laser hits per tree to total leaf area. However, as a consequence of the given range of leaf area measured in the present study, a linear regression model between both parameters was suitable for describing the leaf area of the abundant trees in both orchards. Since canopy light interception determines canopy photosynthesis, the estimation of the fraction of intercepted light by the canopy directly from the LiDAR point cloud for each tree should be explored in future work. For whole canopies, the relationship between total leaf area and the fraction of intercepted light cannot be linear, as the mutual shading of overlapping leaves is disabling the exposure of a large fraction of the inner leaves to saturating light conditions. An increase in the leaf area per tree in a given space allotted to the tree increases this effect. As a consequence, the leaf area necessary to meet the carbon requirements of a fruit with a defined size varies for trees which are different in total leaf area and associated leaf area index (cf. Fig. 8). This may be one explanation for the achieved higher fruit size on Pinova compared to RoHo 3615, despite similar leaf area to fruit ratios and temperatures in the cell division stage. However, the canopy follows seasonal dynamics, as a consequence of vegetative growth, the loss of leaf area through pathogens and in some orchards, summer pruning. Therefore, the leaf area demand per fruit cannot be a constant. On days with low solar radiation and a resulting dramatic rise in the leaf area demand per fruit (Fig. 7e, 7f), the woody structures of the tree have the potential to mobilize carbon reserves to maintain fruit growth for a period of approximately 2 days (McQueen *et al*., 2005). Such a buffering of daily carbon supply has been observed in shading studies as well (Lakso, 2011). Therefore, the smoothing of the seasonal course in LA_{demand} with the Savitzky-Golay filter, led to a more valid general seasonal pattern.

In future studies, the seasonal development of leaf area and light interception per tree should be measured several times over the season in order to visualize seasonal patterns and identify critical periods. In the present trials, a chronological sigmoid course of the total leaf area per tree was assumed, which is generally valid. However, as temperature is a major driver of shoot and leaf development early in the season (Wagenmakers, 1996), the extent of leaf area development in this critical period for fruit development (Lakso and Goffinet, 2017) should be modelled against degree-days or estimated by LiDAR methods at several measuring dates. Fruit thinning should be realized in less than 30 DAFB, when the leaf area of the tree is still developing. Therefore, it is required to estimate the leaf area at full canopy from the measured values, *e.g*., after petal fall. Before petal fall, the leaves and petals may not be distinguished by the LiDAR readings. After petal fall, approximately 40% of the total leaf area of a tree is developed (Lakso, 1984; Forshey *et al*., 1987, Wünsche *et al*., 1996). In order to estimate the final leaf area per tree immediately after petal fall would enable the consideration of the fruit bearing capacity in chemical fruit thinning, which is, depending on the thinning agent, applicable until fruit diameter of 20 mm is reached. After this, fruit becomes insensitive to the currently available thinning agents (McArtney and Obermiller, 2012).

The comparison between LA_{demand} and the measured LA:F of trees in both orchards demonstrated that > 20% of the trees had an LA:F value which was too high. This finding demonstrates that Pinova could potentially bear an additional 1.6 t ha^{-1} and RoHo 361, 3.1 t ha^{-1} more fruit, which is the equivalent of up to 5% of the harvested yields in the orchards, without any negative effect on fruit size. The best fruit size from an economic point of view, however, should be evaluated by each farmer for every orchard and year. The negative relationship between average fruit size and yield per tree is well known. The crop value additionally depends on the specific value-chain and the market situation. Finally, for each variety, the target crop load must not be detrimental to return bloom and sustained cropping. Such economic and tree performance considerations are required to determine the target fruit size, which can lead to the precise calculation of target fruit number per tree. However, a known FBC can support decisions and avoid yield loss.

CONCLUSIONS

1. It was demonstrated that the estimation of the daily leaf area demand per fruit to satisfy its C requirement, LA_{demand}, undergoes seasonal changes. When the foliage of the tree is fully developed, the fruit bearing capacity of the tree may be estimated using LA_{demand} in the period when fruit growth rates achieve their maximum extent.

2. The estimation of the leaf area of individual trees using LiDAR scanning was shown to be feasible to allow for individual tree estimates of target fruit numbers.

3. The fruit bearing capacity of individual trees varied within the orchards investigated. This was due to variation in the total leaf area per tree. Field uniform flower thinning resulted in an avoidable sub-optimal crop load above or below fruit bearing capacity in both orchards. When combined with the modelling of carbon supply and crop carbon demand, the optimal number of fruit may be estimated for each tree.

ACKNOWLEDGEMENTS

We thank Karin Bergt, Thomas Giese and Lutz Günzel for technical support in their orchards, Michael Pflanz for providing the MATLAB script required to estimate individual leaf area from RGB-images of leaves, and Werner B. Herppich for his general advice concerning gas exchange measurements and the evaluation of raw data.

Conflict of interest. The authors declare no conflict of interest

CREDIT AUTHOR STATEMENT

MP: Conceptualization, Software, Formal analysis, Investigation, Methodology, Writing – Original Draft, Visualisation

AL: Methodology, Validation, Formal analysis, Writing – Review & Editing

NT: Methodology, Software, Investigation, Formal analysis

MZ: Conceptualization, Methodology, Writing – Review & Editing, Supervision, Project administration, Funding acquisition

Conflict of interest: The authors declare no conflict of interest.

REFERENCES

Aggelopoulou K.D., Wulfsohn D., Fountas S., Gemtos T.A., Nanos G.D., and Blackmore S., 2010. Spatial variation in yield and quality in a small apple orchard. Precis. Agric., 11, 538-556. https://doi.org/10.1007/s11119-009-9146-9

Arno J., Escola A., Valles J.M., Llorens J., Sanz R., *et al*., 2012. Leaf area index estimation in vineyards using a ground-based LiDAR scanner. Prec. Agr., 14, 290-306. https://doi.org/10.1007/s11119-012-9295-0

Bepete M. and Lakso A.N., 1997. Apple fruit respiration in the field: relationships to fruit growth rate, temperature, and light exposure. Acta Hortic., 451, 319-326. https://doi.org/10.17660/ActaHortic.1997.451.37

Bepete M. and Lakso A.N., 1998. Differential effects of shade on early season fruit and shoot growth rates in 'Empire' apple branches. HortScience, 33, 823-825. https://doi.org/10.21273/HORTSCI.33.5.823

Brandes N. and Zude-Sasse M., 2019. Respiratory patterns of European pear (*Pyrus communis* L. 'Conference') throughout pre- and postharvest fruit development. Heliyon, 5, e01160. https://doi.org/10.1016/j.heliyon.2019.e01160

Breen K.C., Tustin D.S., Palmer J.W., and Close D.C., 2015. Method of manipulating floral bud density affects fruit set responses and productivity in apple. Sci. Hortic.-Amsterdam, 197, 244-253. https://doi.org/10.1016/j.scienta.2015.09.042

Bresilla K., Perulli G.D., Boini A., Morandi B., Corelli Grappadelli L., and Manfrini L., 2019. Single-shot convolution neural networks for real-time fruit detection within the tree. Front. Plant Sci., 611(10), 1-12. https://doi.org/10.3389/fpls.2019.00611

Charles-Edwards DA., 1982. Physiological determinants of crop growth. Academic Press, Sydney.

Corelli-Grappadelli L., Lakso A.N., Flore J.A., 1994. Early season patterns of carbohydrate partitioning in exposed and shaded apple branches. J. Am. Soc. Hortic. Sci., 119, 596-603. https://doi.org/10.21273/JASHS.119.3.596

Doerflinger F.C., Lakso A.N. and Braun P., 2015. Adapting the MaluSim Apple tree model for the 'Gala' cultivar. Acta Hortic., 1068, 267-272. https://doi.org/10.17660/ActaHortic.2015.1068.33

Forshey C.G., Weires R.W., and van Kirk J.R., 1987. Seasonal development of the leaf canopy of 'Macspur McIntosh' apple trees. HortScience, 22, 881-883.

Glenn D.M., 2016. Dry matter partitioning and photosynthetic response to biennial bearing and freeze damage in 'Empire' apple. Sci.Hortic.-Amsterdam, 210, 1-5. https://doi.org/10.1016/j.scienta.2016.06.042

Greene D.W., Lakso A.N., Robinson T.L., and Schwallier P., 2013. Development of a fruitlet growth model to predict thinner response on apples. HortScience, 48, 584-587. https://doi.org/10.21273/HORTSCI.48.5.584

Handschack M. and Schmidt S., 1990. Grafisches Modell zur Beschreibung der Ertragsbildung bei Apfel unter Berücksichtigung von Wechselwirkungen zwischen den Ertragskomponenten. Arch. Gartenbau, 38, 399-405.

Hansen P., 1967. 14C-studies on apple trees. I. The effect of the fruit on the translocation and distribution of photosynthates. Physiol. Plant., 20, 382-91. https://doi.org/10.1111/j.1399-3054.1967.tb07178.x

Hansen P., 1969. 14C-Studies on apple trees. IV. Photosynthate consumption in fruits in relation to the leaf-fruit ratio and to the leaf-fruit position. Physiol. Plant., 22, 186-198. https://doi.org/10.1111/j.1399-3054.1969.tb07855.x

Hobart M., Pflanz M., Weltzien C., and Schirrmann M., 2020. Growth Height Determination of Tree Walls for Precise Monitoring in Apple Fruit Production Using UAV Photogrammetry. Remote Sensing, 12(10), 1656, 1-17. https://doi.org/10.3390/rs12101656

Iwanami H., Moriya-Tanaka Y., Honda C., Hanada T., and Wada M., 2018. A model for representing the relationships among crop load, timing of thinning, flower bud formation, and fruit weight in apples. Sci. Hortic.-Amsterdam, 242, 181-187. https://doi.org/10.1016/j.scienta.2018.08.001

Jackson J.E. and Palmer J.W., 1980. A computer model study of light interception by orchards in relation to mechanised harvesting and management. Sci. Hortic.-Amsterdam., 13, 1-7. https://doi.org/10.1016/0304-4238(80)90015-1

Janoudi A. and Flore J.A., 2005. Application of ammonium thiosulfate for blossom thinning in apples. Sci. Hortic.-Amsterdam, 104, 161-168. https://doi.org/10.1016/j.scienta.2004.08.016

Jones H.G., 1981. Carbon dioxide exchange of developing apple (*Malus pumila* Mitt.) fruits. J. Exp. Bot., 32, 1203-1210. https://doi.org/10.1093/jxb/32.6.1203

Kofler J., Milyaev A., Capezzone F., Stojnić S., Mićić N., *et al*., 2019. High crop load and low temperature delay the onset of bud initiation in apple. Sci. Rep., 9, 17986 (2019). https://doi.org/10.1038/s41598-019-54381-x

Koike H., Yoshizawa S., and Tsukahara K., 1990. Optimum crop load and dry weight partitioning in Fuji/M.26 apple trees. J. Jap. Soc. Hort. Sci., 58, 827-834. https://doi.org/10.2503/jjshs.58.827

Lakso A.N., 1984. Leaf area development patterns in young pruned and unpruned apple trees.J. Amer. Soc. Hort. Sci., 109, 861-865.

Lakso A.N., 2011. Early fruit growth and drop - the role of carbon balance in the apple tree. Acta Hortic., 903, 733-742. https://doi.org/10.17660/ActaHortic.2011.903.102

Lakso A.N., Corelli Grappadelli L., Barnard J., and Goffinet M.C., 1995. An expolinear model of the growth pattern of the apple fruit. J. Hort. Sci., 70(4), 389-394. https://doi.org/10.1080/14620316.1995.11515308

Lakso A.N., Piccioni R.M., Denning S.S., Sottile F., and Costa Tura J., 1999. Validating an apple dry matter production model with whole canopy gas exchange measurements in the field. Acta Hortic., 499, 115-122. https://doi.org/10.17660/ActaHortic.1999.499.11

Lakso A.N., White M.D., and Tustin D.S., 2001. Simulation modeling of the effects of short and long-term climatic variations on carbon balance of apple trees. Acta Hortic., 557, 473-480. https://doi.org/10.17660/ActaHortic.2001.557.63

Lakso A.N., Greene D.W., and Palmer J.W., 2006. Improvements on an apple carbon balance model. Acta Hortic., 707, 57-61. https://doi.org/10.17660/ActaHortic.2006.707.6

Lakso A.N. and Johnson R.S., 1990. A simplified dry matter production model for apple using automatic programming simulation software. Acta Hortic., 276, 141-148. https://doi.org/10.17660/ActaHortic.1990.276.15

Lakso A.N. and Robinson T.L., 2014. Integrating physiological models in applied fruit crop research. Acta Hortic., 1058, 285-290. https://doi.org/10.17660/ActaHortic.2014.1058.33

Lakso A.N. and Goffinet M.C., 2017. Advances in understanding apple fruit development. In: Achieving sustainable cultivation of apples (Ed. K. Evans), Burleigh Dodds Science Publishing, Cambridge, United Kingdom.

Ligges U., Short T., Kienzle P., *et al.*, 2015. Package 'signal'. R Foundation for Statistical Computing.

Lopez G., Boini A., Manfrini L., Torres-Ruiz J.M., Pierpaoli E., Zibordi M., and Corelli-Grappadelli L., 2018. Effect of shading and water stress on light interception, physiology and yield of apple trees. Agr. Water Manag., 210, 140-148. https://doi.org/10.1016/j.agwat.2018.08.015

McArtney S.J. and Obermiller J.D., 2012. Use of 1-Aminocyclopropane carboxylic acid and metamitron for delayed thinning of apple fruit. Hortscience, 47, 1612-1616. https://doi.org/10.21273/HORTSCI.47.11.1612

Manfrini L., Taylor J.A., and Corelli-Grappadelli L., 2009. Spatial analysis of the effect of fruit thinning on apple crop load. Eur. J. Hor. Sci., 74(2), 54-60. http://www.pubhort.org/ejhs/2009/file_968077.pdf

McCree K.J., 1972. Test of current definitions of photosynthetically active radiation against leaf photosynthesis data. Agr. Meteorol., 10, 443-53. https://doi.org/10.1016/0002-1571(72)90045-3

McQueen J.C., Minchin P.E.H., Thorpe M.R., Silvester W.B., 2005. Short-term storage of carbohydrate in stem tissue of apple (Malus domestica), a woody perennial: evidence for involvement of the apoplast. Funct. Plant Biol., 32, 1027-1031. https://doi.org/10.1071/FP05082

Mirás-Avalos J.M., Egea G., Nicolas E., *et al*., 2011. QualiTree, a virtual fruit tree to study the management of fruit quality. II. Parameterisation for peach, analysis of growth-related processes and agronomic scenarios. Trees, 25, 785-799. https://doi.org/10.1007/s00468-011-0555-9

Monteith J.L., 1977. Climate and the efficiency of crop production in Britain. Philos. Trans. R. Soc. Lond., Ser. B, 281, 277-294. https://doi.org/10.1098/rstb.1977.0140

Musacchi S. and Serra S., 2018. Apple fruit quality: overview on pre-harvest factors. Sci. Hortic.-Amsterdam, 234, 409-430. https://doi.org/10.1016/j.scienta.2017.12.057

Pallas B., Da Silva D., Valsesia P., Yang W., Guillaume O., *et al*., 2016. Simulation of carbon allocation and organ growth variability in apple tree by connecting architectural and source-sink models. Ann. Bot., 118, 317-330. https://doi.org/10.1093/aob/mcw085

Palmer J.W., 1992. Effects of varying crop load on photosynthesis, dry matter production and partitioning of Crispin/M.27 apple trees. Tree Physiol., 11, 19-33. https://doi.org/10.1093/treephys/11.1.19

Palmer J.W., Giuliani R., and Adams H.M., 1997. Effect of crop load on fruiting and leaf photosynthesis of 'Braeburn'/M.26 apple trees. Tree Physiol., 17, 741-746. https://doi.org/10.1093/treephys/17.11.741

Palmer J.W., Wünsche J.N., Meland M., and Hann A., 2002. Annual dry matter production by three apple cultivars at four within-row spacings in New Zealand. J. Hort. Sci. Biotechnol., 77, 712-717. https://doi.org/10.1080/14620316.2002.11511561

Pavel E.W. and DeJong T.M., 1995. Seasonal patterns of non-structural carbohydrates of apple (*Malus pumila* Mill.) fruits: relationship with relative growth rates and contribution to solute potential. J. Hort. Sci., 70, 127-134. https://doi.org/10.1080/14620316.1995.11515282

Penzel M. and Kröling C., 2020. Thinning efficacy of metamitron on young 'RoHo 3615' (Evelina®) apple. Sci. Hortic.-Amsterdam, 272, 1-6. https://doi.org/10.1016/j.scienta.2020.109586.

Penzel M., Pflanz M., Gebbers R., and Zude-Sasse M., 2020. Tree adapted mechanical flower thinning prevents yield loss caused by over thinning of trees with low flower set in apple. Eur. J. Hort. Sci., 2021 (in press).

R Core Team, **2018.** R: A language and environment for statistical computing. R Foundation for Statistical Computing, Vienna, Austria. https://www.R-project.org/

Robinson T.L., Lakso A.N., and Greene D., 2017. Precision crop load management: The practical implementation of physiological models. Acta Hortic., 1177, 381-390. https://doi.org/10.17660/ActaHortic.2017.1177.55

Schechter I., Proctor J.T.A., and Elfving D.C., 1993. Characterization of seasonal fruit growth of 'Idared' apple. Sci. Hortic.-Amsterdam, 54, 203-210. https://doi.org/10.1016/0304-4238(93)90088-8

Schumacher R., 1962. Fruchtentwicklung und Blütenknospenbildung beim Apfel in Abhängigkeit von der Blattmasse, unter Berücksichtigung der abwechselnden Tragbarkeit. Ph.D. Thesis, ETH Zürich. https://doi.org/10.3929/ethz-a-000088562

Skene D.S., 1966. The distribution of growth and cell division in the fruit of Cox's Orange Pippin. Ann. Bot., 30(3), 493-512. https://doi.org/10.1093/oxfordjournals.aob.a084092

Stanley C.J., Tustin D.S., Lupton G.B., McArtney S., Cashmore W.M., and De Silva H.N., 2000. Towards understanding the role of temperature in apple fruit growth response in three geographical regions within New Zealand. J. Hortic. Sci. Biotech., 75(4), 413-422. https://doi.org/10.1080/14620316.2000.11511261

Treder W., 2008. Relationship between yield, crop density coefficient and average fruit weight of 'Gala' apple. J. Fruit Orn. Plant Res., 16, 53-63

Tsoulias N., Paraforos D.S., Fountas S., and Zude-Sasse M., 2019. Estimating canopy parameters based on the stem position in apple trees using a 2D LiDAR. Agronomy, 9(11), 740, 1-18. https://doi.org/10.3390/agronomy9110740

Tsoulias N., Paraforos D.S., Xanthopoulos G., Zude-Sasse M., 2020. Apple shape detection based on geometric and radiometric features using a LiDAR laser scanner. Remote Sensing, 12, 2481. https://doi.org/10.3390/rs12152481

Vanbrabant Y., Delalieux S., Tits L., Pauly K., Vandermaesen J., and Somers B., 2020. Pear Flower Cluster Quantification Using RGB Drone Imagery. Agronomy, 10, 407, 1-26. https://doi.org/10.3390/agronomy10030407

Wagenmakers P.S., 1996. Effects of light and temperature on potential apple production. Acta Hortic., 416, 191-198. https://doi.org/10.17660/ActaHortic.1996.416.23

Walton E.F., Wünsche J.N., and Palmer J.W., 1999. Estimation of the bioenergetic costs of fruit and other organ synthesis in apple. Physiol. Plant., 106, 129-134. https://doi.org/10.1034/j.1399-3054.1999.106118.x

Warrington I.J., Faulton T.A., Halligan E.A., and de Silva H.N., 1999. Apple fruit growth and maturity are affected by early season temperatures. J. Amer. Soc. Hort. Sci., 124, 468-477. https://doi.org/10.21273/JASHS.124.5.468

Wójcik P., Rutkowski K., and Treder W., 2001. Quality and storability of 'Gala' apples as affected by crop load. Folia Hortic., 13(2), 89-96

Wünsche J.N., Lakso A.N., Robinson T.L., Lenz F., and Denning S.S., 1996. The bases of productivity in apple production systems: the role of light interception by different shoot types. J. Amer. Soc. Hort. Sci., 121, 886-893. https://doi.org/10.21273/JASHS.121.5.886

Xia G., Cheng L., Lakso A.N., and Goffinet M., 2009. Effects of nitrogen supply on source-sink balance and fruit size of 'Gala Apple' trees. Hort. Sci., 134, 126-133. https://doi.org/10.21273/JASHS.134.1.126

Yoder K.S., Peck G.M., Combs L.D., and Byers R.E., 2013. Using a pollen tube growth model to improve apple blossom thinning for organic production. Acta Hortic., 1001, 207-214. https://doi.org/10.17660/ActaHortic.2013.1001.23